

ARTICLE

Open Access

# Psychiatric polygenic risk associates with cortical morphology and functional organization in aging

Annie Lee<sup>1</sup>, Mojun Shen<sup>2</sup> and Anqi Qiu<sup>1,2,3</sup> 

## Abstract

Common brain abnormalities in cortical morphology and functional organization are observed in psychiatric disorders and aging, reflecting shared genetic influences. This preliminary study aimed to examine the contribution of a polygenic risk for psychiatric disorders (PRS<sub>cross</sub>) to aging brain and to identify molecular mechanisms through the use of multimodal brain images, genotypes, and transcriptome data. We showed age-related cortical thinning in bilateral inferior frontal cortex (IFC) and superior temporal gyrus and alterations in the functional connectivity between bilateral IFC and between right IFC and right inferior parietal lobe as a function of PRS<sub>cross</sub>. Interestingly, the genes in PRS<sub>cross</sub>, that contributed most to aging neurodegeneration, were expressed in the functionally connected cortical regions. Especially, genes identified through the genotype-functional connectivity association analysis were commonly expressed in both cortical regions and formed strong gene networks with biological processes related to neural plasticity and synaptogenesis, regulated by glutamatergic and GABAergic transmission, neurotrophin signaling, and metabolism. This study suggested integrating genotype and transcriptome with neuroimage data sheds new light on the mechanisms of aging brain.

## Introduction

Normal brain aging is a complex process associated with structural and functional alterations. However, such alterations are not exclusive to advancing age but also to psychiatric disorders<sup>1–6</sup>. Covariance of brain alterations in aging and psychiatric disorders may reflect shared genetic influences and underlying common molecular processes. In this study, we aimed to examine the contribution of psychiatric risk genes to aging brain and to identify common biological processes through the use of multimodal brain images, genotypes, and gene transcriptome profiles.

There is substantial evidence on age-related alterations at the levels of individual structures and neural networks.

At an anatomical level, prominent cortical thinning in the prefrontal and parietal cortices and relatively sparse cortical thinning in the temporal and occipital cortices are observed in older adults<sup>7–12</sup>. On the other hand, resting-state fMRI (rs-fMRI) is used to examine brain functional organization at a system level based on the synchronization of resting-state blood-oxygen-level-dependent signals among brain regions<sup>13</sup>. Age is associated with decreased functional connectivity among the central hub regions of the brain, specifically the frontotemporal and frontoparietal functional connectivity<sup>14,15</sup>. Inquisitively, remarkably similar trends of age-related cortical thinning and functional connectivity alterations are observed in patients with psychiatric disorders, including schizophrenia, bipolar disorder, major depression disorder etc.<sup>1–6,16–18</sup>. Meta-analysis reveals gray matter loss in the prefrontal cortex converged across multiple psychiatric disorders. In parallel, the common gray matter loss regions form functional networks that are associated with deficits in executive function observed across psychiatric disorders

Correspondence: Anqi Qiu ([bieqa@nus.edu.sg](mailto:bieqa@nus.edu.sg))

<sup>1</sup>Department of Biomedical Engineering, National University of Singapore, Singapore 117576, Singapore

<sup>2</sup>Singapore Institute for Clinical Sciences, The Agency for Science, Technology and Research, Singapore 117609, Singapore

Full list of author information is available at the end of the article

© The Author(s) 2017



**Open Access** This article is licensed under a Creative Commons Attribution 4.0 International License, which permits use, sharing, adaptation, distribution and reproduction in any medium or format, as long as you give appropriate credit to the original author(s) and the source, provide a link to the Creative Commons license, and indicate if changes were made. The images or other third party material in this article are included in the article's Creative Commons license, unless indicated otherwise in a credit line to the material. If material is not included in the article's Creative Commons license and your intended use is not permitted by statutory regulation or exceeds the permitted use, you will need to obtain permission directly from the copyright holder. To view a copy of this license, visit <http://creativecommons.org/licenses/by/4.0/>.

and aging<sup>19,20</sup>. These findings emphasize the importance of morphology of neural substrates and their corresponding functional organization shared across psychopathology and aging.

The common morphological and functional alterations in aging and psychiatric disorders may in part be due to shared genetic influences. Indeed, genome-wide association studies (GWAS) identify common variants associated with brain morphology in older adults<sup>21,22</sup> and several of these common variants are found to be associated with psychiatric disorders<sup>23,24</sup>. Alternatively, candidate genetic association studies also reveal the moderation role of psychiatric risk genes in the relationship of morphological and functional alterations with age. For instance, genetic variants of COMT val158met and Disrupted in Schizophrenia 1 (DISC1) modulate age-related prefrontal and parietal cortical thinning<sup>25</sup>. Interestingly, the functional connectivity between the prefrontal and parietal regions is also manipulated by genetic variants of COMT and DISC1<sup>26–30</sup>. Nevertheless, candidate gene approaches or GWAS bear weaknesses and gene products operate in networks, such that alterations in neural systems that increase vulnerability for psychopathology derive from genomic variants at multiple sites and may converge to influence common biological systems. Indeed, psychiatric disorders and aging are polygenic traits in nature<sup>31,32</sup>. The genetic susceptibility to psychiatric disorders and aging appears to reflect the cumulative influence of multiple genetic variants<sup>33</sup>. This idea leads to the use of methods of genomic risk profiling to examine the influence of genetic burden as reflected by a set of “risk” alleles for across psychiatric disorders<sup>34</sup>. Existing GWAS for cross psychiatric disorders (Cross-Disorder Group of the Psychiatric Genomics Consortium, 2013) make it feasible to access the risk alleles and effect sizes of SNPs and facilitate the computation of polygenic risk for characterizing accumulative genetic risks for cross psychiatric disorders. Inquisitively, psychiatric-related genes are also over-represented in the gene set related to aging<sup>35</sup>. This concordance therefore emphasizes the significance of studying polygenic architecture across multiple psychiatric disorders to understand its role and biological processes in aging.

In this study, we aimed to compute a polygenic risk score of cross psychiatric disorders ( $PRS_{cross}$ ) for each individual in a Chinese sample comprised of adults aged 21 years and above, as the sum of the count of risk alleles weighted by the effect size in the discovery sample obtained from existing GWAS on cross psychiatric disorders (Cross-Disorder Group of the Psychiatric Genomics Consortium, 2013). We then aimed to examine whether  $PRS_{cross}$  moderates age effects on cortical thickness and its parallel functional organization assessed using both structural and rs-fMRI. Based on the aforementioned

genetic influences on the brain in psychiatric disorders and aging, we hypothesized that  $PRS_{cross}$  would modulate associations of age with cortical thickness, particularly in the prefrontal and parietal cortex, and functional connectivity between these two regions.

Furthermore, we aimed to identify genes involved in the computation of  $PRS_{cross}$  that were most contributed to the modulation effects on age-related alterations in cortical thickness and its functional organization and explore their biological processes. Recent studies observed the similarity of the cortical topological organization identified based on rs-fMRI and transcriptome data<sup>36,37</sup>, suggesting the potential use of imaging genetics (combination of genotype and rs-fMRI) for understanding molecular basis supporting cortical functional organization. In this study, we further took advantage of the available brain transcriptome database<sup>38</sup> and aimed (1) to identify genes with common gene expression profiles in the cortical regions whose thickness or functional connectivity was as a function of age by gene interaction; (2) to investigate biological processes formed by this set of genes using weighted gene co-expression network analysis (WGCNA)<sup>39</sup> and gene ontology enrichment analysis. The transcriptome analysis evaluated validity of the age by gene interaction effects on the cortical morphology and functional organization. Overall, covariance in biological processes found by genotype–brain associations and the unique transcriptional signature of the cortical morphology and cortico-cortical organization may provide convergent understanding of biological processes in aging.

## Material and methods

### Subjects

Two hundred and fourteen healthy Singaporean Chinese volunteers aged from 21 to 80 years old were recruited (males: 93; females: 121) for this study. Volunteers with the following conditions were excluded: (1) major illnesses/surgery (heart, brain, kidney, lung surgery); (2) neurological or psychiatric disorders; (3) learning disability or attention deficit hyperactive disorder; (4) head injury with loss of consciousness; (5) non-removable metal objects on/in the body such as a cardiac pacemaker; (8) diabetes or obesity; (9) a MMSE score of less than 24<sup>40</sup>. This study was approved by the National University of Singapore Institutional Review Board and all participants provided written informed consent prior to participation.

### MRI data acquisition

MRI scans were acquired using a 3 T Siemens Magnetom Trio Tim scanner with a 32-channel head coil at the Clinical Imaging Research Centre of the National University of Singapore. The image protocols were (i) high-resolution isotropic T<sub>1</sub>-weighted Magnetization Prepared Rapid Gradient Recalled Echo (MPRAGE; 192 slices, 1

mm thickness, sagittal acquisition, field of view  $256 \times 256$  mm, matrix =  $256 \times 256$ , repetition time = 2300 ms, echo time = 1.90 ms, inversion time = 900 ms, flip angle =  $9^\circ$ ); (ii) isotropic axial resting-state functional MRI imaging protocol (single-shot echo-planar imaging; 48 slices with 3 mm slice thickness, no inter-slice gaps, matrix =  $64 \times 64$ , field of view =  $192 \times 192$  mm, repetition time = 2300 ms, echo time = 25 ms, flip angle =  $90^\circ$ , scanning time = 8.01 min). During the rs-fMRI scan, the subjects were asked to close their eyes. The image quality was checked through visual inspection after the acquisition while subjects were still in scanner. If the motion of the image was large, the scan was repeated. However, the image was removed from the study if the motion of the image remains large after 3 repetitions.

### MRI data preprocessing

#### Structural MRI analysis

In the structural  $T_1$ -weighted MRI analysis, gray matter, white matter, cerebral spinal fluid (CSF), lateral ventricles, and subcortical structures were automatically segmented from the intensity-inhomogeneity corrected  $T_1$ -weighted MR images<sup>41</sup>. For cortical thickness analysis, an inner surface was constructed at the boundary between white and gray matter and then propagated to an outer surface at the boundary between gray matter and CSF. Cortical thickness was measured as the distance between the corresponding points on the inner and outer surfaces<sup>42</sup>. A cortical surface mapping algorithm, large deformation diffeomorphic metric mapping (LDDMM), was then applied to align individual cortical surfaces to an atlas cortical surface for group analysis of cortical thickness<sup>43</sup>.

#### Rs-fMRI network analysis

The rs-fMRI data were first processed with slice timing, motion correction, skull stripping, and grand mean scaling of the data (to whole brain modal value of 100). Within each subject, the rs-fMRI images were aligned to the  $T_1$ -weighted image. six parameters of head motion and CSF and white matter signals were regressed out from the rs-fMRI signals. The functional signals were then band-pass filtered (0.01–0.08 Hz). Finally, the fMRI data were represented on the cortical surface (Qiu et al. 2006) and transformed to the atlas cortical surface based on the LDDMM transformation mentioned above. To quantify the quality of rs-fMRI data in terms of head motion, framewise displacement due to motion averaged over the image volume was calculated for individual subjects. Its mean and standard deviation were respectively 0.057 and 0.033 mm among all the subjects used in this study. The head motion was independent of age ( $p > 0.05$ ).

### Genotyping and $PRS_{cross}$ computation

Saliva was collected from each participant through the Oragene DNA Self-Collection Kit (DNA Genotek Inc., Kanata, Ontario, Canada). The samples were genotyped on Illumina Omni express arrays, recently shown to perform well and have better coverage than competitors in Asian populations<sup>44</sup> and on Illumina Exome arrays as well as Taqman array, following the manufacturer's instructions by Expression Analysis Inc. Data were processed in GenomeStudio Genotyping Module<sup>TM</sup>. Genotyping calls were made by the GenCall software which incorporates a clustering algorithm (GenTrain) and a calling algorithm (Bayesian model). The GenCall score of each SNP probe was generated to rank and filter out failed genotypes<sup>45</sup>. In this study, the genotypes with a GenCall score of less than 0.15 were not assigned genotypes<sup>45</sup>. All SNPs in this study did not deviate from the Hardy-Weinberg equilibrium (HWE,  $p < 0.001$ )<sup>46</sup>.

The  $PRS_{cross}$  was computed based on genotyping data of the subjects in this study and meta-analysis results from the Psychiatric Genomics Consortium (PGC) using plink (Cross-Disorder Group of the PGC, 2013) The  $PRS_{cross}$  was a cumulative summary score computed as the sum across the allelic scoring system (0, 1, and 2) of the SNPs of individual weighted by odd ratio (OR) of the risk SNPs. ORs were obtained from the meta-analysis on GWAS on cross-psychiatric disorders (autism spectrum disorder, attention deficit-hyperactivity disorder, bipolar disorder, major depressive disorder, and schizophrenia; <http://www.med.unc.edu/pgc>). The risk SNPs were selected at several p-value levels (0.01, 0.05, 0.10, 0.15, and 0.20). The resulting numbers of SNPs for  $PRS_{cross}$  were 8645, 30518, 54353, 76383 and 97821, respectively. The  $PRS_{cross}$  were then standardized to a mean of zero and standard deviation of one.

### Statistical analysis

Age by  $PRS_{cross}$  interaction on cortical thickness and rs-fMRI functional connectivity was performed using Surfstat<sup>47</sup>.

#### Cortical thickness

Regression analysis was used to examine age by  $PRS_{cross}$  interaction on cortical thickness, where age,  $PRS_{cross}$  and the interaction of their mean-centered measures were included as main factors and gender as a covariate. Age was considered as a continuous variable. Results at each surface vertex were thresholded at a level of significance ( $p < 0.005$ ) and were corrected for multiple comparisons at a cluster level of significance ( $p < 0.05$ ). In post hoc analysis, age effects on thickness were examined in low and high genetic risk groups. For this, the sample was divided into two groups,  $PRS_{cross} < 0$  (low) and  $PRS_{cross} > 0$  (high). Thickness was averaged in each cortical cluster with significant age by  $PRS_{cross}$  interaction and considered as dependent variable in post hoc regression analysis. Age

was used as main factor and gender as covariate. Slope analysis was further employed to compare the slopes of age-related decline in cortical thickness between the two PRS<sub>cross</sub> groups. The second post hoc analysis examined whether the PRS<sub>cross</sub> plays the same role in young (20–39 years old), middle (40–54 years old), and old adults (55 and above). Pairwise group comparison analysis was performed on thickness with the PRS<sub>cross</sub> as a main factor in each age group. All post hoc analyses were run separately for individual brain regions.

### Resting state fMRI (rs-fMRI)

To examine age by PRS<sub>cross</sub> interaction on the functional connectivity of the cortical regions identified above, seed-based correlation analysis was used to generate the functional connectivity map of these cortical regions. One-sample Student's *t*-test was then used to create a group-level functional connectivity map where each surface vertex was thresholded at a level of significance ( $p < 0.005$ ) and then corrected for multiple comparisons at a cluster level of significance ( $p < 0.05$ ).

Subsequently, regression models were used to examine age by PRS<sub>cross</sub> interaction on the functional connectivity maps obtained from the seed-based correlation analysis. Age, PRS<sub>cross</sub> and their interaction were included as main factors and gender as a covariate. Age was considered as a continuous variable. Results at each surface vertex were thresholded at the level of significance ( $p < 0.005$ ) and corrected for multiple comparisons at the cluster level of significance ( $p < 0.05$ ). The aforementioned post hoc analyses on thickness were also carried out for the functional connectivity with significant age by PRS<sub>cross</sub> interaction.

### Analysis of biological processes for cortical morphology

Our study aimed to identify underlying biological processes for age by PRS<sub>cross</sub> interaction on cortical thickness. For this, gene transcriptome data of six healthy adult human brains were first extracted from the Allen Brain Atlas database (<http://www.brain-map.org>) in the brain regions whose cortical thickness was shown with age by gene interaction in this study. Second, SNPs (top 10%) involved in the PRS<sub>cross</sub> computation that most contributed age by gene interaction on thickness and were then mapped to genes using the batch query function in UCSC Genome Bioinformatics (<http://genome.ucsc.edu>). Third, this set of genes that express in a particular cortical region was identified and was examined whether they are representative over the set of genes obtained from the age by gene interaction analysis using hypergeometric testing. Fourth, weighted gene co-expression network analysis, a systems biology analysis method, (WGCNA<sup>39</sup>), was used to identify modules of co-expressed genes that correspond to shared functions, such as biological processes. To determine the robustness and reproducibility of each

genetic module and whether the module obtained is significantly better than a random sample of genes, module preservation statistical analysis from WGCNA package was carried out<sup>39</sup>. Two types of network-based module preservation statistics were computed, namely (1) module density-based statistic that determines whether genes remain highly connected in the test set and (2) connectivity-based statistic that determines the extent to which connectivity patterns between genes in the test set remain similar when compared with the training set. In each preservation statistic, *Z* statistics that followed standard normal distribution ( $Z = \frac{\text{observed} - \text{mean}_{\text{permuted}}}{\text{sd}_{\text{permuted}}}$ ) was computed from the permutation test. Subsequently, individual *Z* scores were summarized into a composite measure called Preservation *Z*-score. Preservation *Z*-score greater than 10 indicates strong evidence for the module preservation in the test data set while Preservation *Z*-score less than 2 indicates no evidence of the module preservation. Enrichment analysis on Gene Ontology (GO) terms was further used to explore biological processes of each gene module and Fischer's exact *p*-value (FDR corrected) was reported.

### Transcriptome and gene differential expression analysis

In this study, we assumed that genes with common expression profiles between two cortical regions provide molecular basis for the functional organization of these regions. The gene expression data were extracted for the brain regions whose functional connectivity was significantly influenced by age by PRS<sub>cross</sub> interaction. For a given gene with multiple probes, the expression values were averaged across the probes. A total of 1505 genes of 22 samples in the left IFC and 1505 genes of 6 samples in the right IFC were curated for right IFC-left IFC functional connectivity, and 1150 genes of 6 samples and 1150 genes of 11 samples in the right IPL were curated for right IFC-right IPL functional connectivity. MaxT in bioconductor R package<sup>48</sup> was used to identify the subset of the above extracted genes with no significant differential expression between two brain regions. To further verify whether the genes selected by maxT have similar gene expression patterns in these two brain regions, Kolmogorov-Smirnov test based on mean (KS test) and variance (RKS test) were employed to test for no presence of differences in shift and no differences in variance or scale of the gene set in two brain regions<sup>49,50</sup>. Moreover, hypergeometric test was used to examine whether this commonly expressed gene set is representative over the gene set that most contributed to age by gene on the functional connectivity of these two brain regions. If this gene subset is over-representative, their biological processes were further explored using WGCNA and GO enrichment analysis as described above.



Results

Demographics

Among 214 recruited subjects, 30 subjects with no genetic data and 32 with missing structural MRI or rs-MRI data were excluded, resulting in a final sample size of 174 in this study. Table 1 lists the distribution of age, sex, education level and the Mini-Mental State Examination (MMSE) score in each decade.

Age by PRS<sub>cross</sub> on cortical morphology

Regression analysis was applied to examine age by PRS<sub>cross</sub> interaction on cortical thickness after adjusting for gender. Age by PRS<sub>cross</sub> effects on cortical thickness were observed predominantly in the left inferior frontal

cortex (IFC) (corrected cluster  $p < 0.001$ ), right IFC (corrected cluster  $p = 0.035$ ) and right posterior region of superior temporal gyrus (STG) (corrected cluster  $p = 0.002$ ) (Fig. 1a) with the largest interaction effect at PRS<sub>cross</sub> of  $p = 0.01$  among the five thresholds (0.01, 0.05, 0.10, 0.15, and 0.2). Post-hoc analysis was carried out to further examine the effect of age on cortical thickness of the aforementioned brain regions in low and high genetic risk groups respectively. Age was found to be negatively associated with cortical thickness in the bilateral IFC and posterior region of STG in the low PRS<sub>cross</sub> ( $< 0$ ) group. The high PRS<sub>cross</sub> ( $> 0$ ) group showed that age was negatively associated with cortical thickness in the right posterior segment of STG but not the bilateral IFC

Table 1 Demographics

Age Range	20s (n=34) mean (SD)	30s (n=20) mean (SD)	40s (n=24) mean (SD)	50s (n=42) mean (SD)	60s (n=51) mean (SD)
Female, %	47.1	55.0	66.7	57.1	58.8
Age	24.9 (1.78)	34.0 (2.21)	44.2 (2.90)	54.6 (3.12)	67.6 (4.55)
Education Level	4.62 (0.55)	4.65 (0.59)	3.49(1.10)	3.12 (1.06)	2.51 (1.57)
MMSE scores	29.2(0.97)	28.5 (1.65)	28.1(1.28)	28.1 (1.52)	27.6 (1.92)

Note: Education Level: 0 = no education, 1 = primary school level, 2 = secondary school level, 3 = Singapore – Cambridge General Certificate of Education Ordinary Level (“O” level) / Singapore- Cambridge General Certificate of Education Normal (Academic) Level (“N” level), 4 = Pre-University/Diploma/ITE/Certificate, 5 = Degree and above

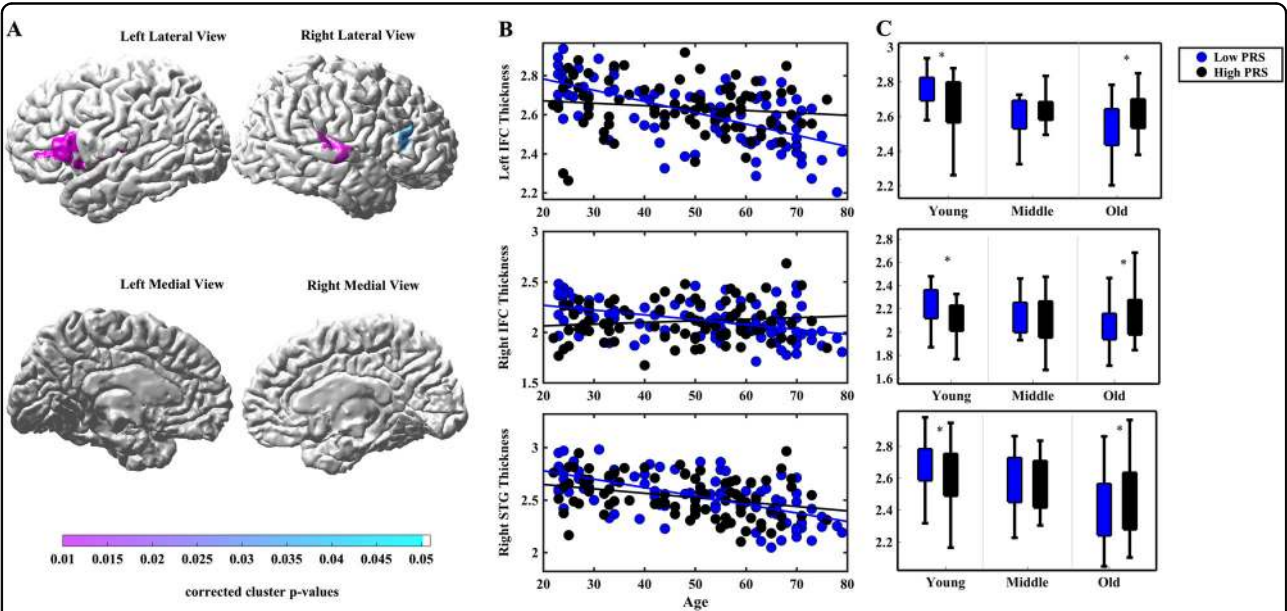


**Fig. 1** Statistical maps of age by PRS<sub>cross</sub> interaction on cortical thickness. Panel **a** shows statistical maps of age by PRS<sub>cross</sub> interaction on cortical thickness. Panel **b** illustrates scatter plots for the relationship of age and cortical thickness in low PRS<sub>cross</sub> ( $< 0$ ) and high PRS<sub>cross</sub> ( $> 0$ ) groups. Panel **c** illustrates boxplots of cortical thickness between low and high PRS<sub>cross</sub> groups in each age group respectively. \*  $p < 0.05$

(Table 2; Fig. 1b). Slope analysis showed a faster decline in age-related cortical thinning of the bilateral IFC and right posterior segment of STG in the low PRS<sub>cross</sub> group as compared to the high PRS<sub>cross</sub> group (column 4 in Table 2).

Figure 1c shows boxplots of cortical thickness between the low and high PRS<sub>cross</sub> groups in young, middle, and old adults. Among the young adults (20–39 years old), the low PRS<sub>cross</sub> group showed thicker cortex in the bilateral IFC and right posterior segment of STG (marginally significant) as compared to the high PRS<sub>cross</sub> group. Among the middle-age adults (40–54 years old), there was no significant difference between the low and high PRS<sub>cross</sub> groups in all the three brain regions ( $p > 0.05$ ). In contrast, among the old adults (55 and above), the low PRS<sub>cross</sub> group showed thinner cortex in the left IFC, right IFC (marginally significant) and right posterior segment of STG as compared to the high PRS<sub>cross</sub> group (column 5 in Table 2).

#### Age by PRS<sub>cross</sub> on functional connectivity

Recent studies suggest that brain regions with age-related gray matter loss and disruptions in their functional connectivity contribute to age-related deficits in executive function<sup>19,20</sup>. We further examined whether PRS<sub>cross</sub> moderated age effects on the functional connectivity of the cortical regions identified above. Figure 2 shows the functional connectivity maps of the bilateral IFC and right posterior segment of STG. The left IFC functionally connected with the bilateral superior frontal gyrus (SFG), middle frontal gyrus (MFG), IFC, precentral gyrus, postcentral gyrus, insula, STG, posterior segment of middle temporal gyrus (MTG), anterior cingulate (ACC) as well as posterior cingulate cortex (PCC) and temporal pole of the right hemisphere (Fig. 2a). Likewise, the right IFC showed functional connections with the bilateral STG, MFG, IFC, posterior region of STG and MTG, inferior parietal lobe (IPL), insula, PCC and precuneus (Fig. 2b). The right posterior region of STG had functional connections with the bilateral IFC, bilateral SFG, IFC, precentral gyrus, postcentral gyrus, STG, MTL, ACC, PCC, occipital and inferior temporal lobe of the right hemisphere (Fig. 2c).

Regression analysis was subsequently used to examine whether PRS<sub>cross</sub> moderates age effects on the above functional connectivity maps. Figure 3a illustrated age by PRS<sub>cross</sub> interaction on the functional connectivity of right IFC-left IFC (corrected cluster  $p = 0.024$ ) as well as between right IFC-right inferior parietal lobe (IPL) (corrected cluster  $p = 0.016$ ) with the greatest interaction effects at PRS<sub>cross</sub> of  $p = 0.15$  and  $p = 0.10$  among the five thresholds (0.01, 0.05, 0.10, 0.15 and 0.2), respectively. Further post-hoc analysis showed that in the low PRS<sub>cross</sub> group, age was negatively associated with the functional connectivity of right IFC with left IFC and right

IPL. In contrast, the high PRS<sub>cross</sub> group did not show any association between age and the functional connectivity of right IFC-left IFC and right IFC-right IPL. Slope analysis showed a faster rate of decline in the functional connectivity of right IFC-left IFC and right IFC-right IPL in the low PRS<sub>cross</sub> group as compared to the high PRS<sub>cross</sub> group (column 4 in Table 2; Fig. 3b).

Figure 3c shows boxplots of the functional connectivity of the two PRS<sub>cross</sub> groups in young, middle, and old adults. Among the young adults, the low PRS<sub>cross</sub> group showed stronger functional connectivity between right IFC-right IFC and right IFC-right IPL compared to the high PRS<sub>cross</sub> group. Among the middle and old-age groups, there was no significant difference between the two PRS<sub>cross</sub> groups in the functional connectivities of right IFC-right IFC and right IFC-right IPL ( $p > 0.05$ ) (Table 2 column 5).

#### Biological processes for age by gene interaction on cortical thickness

Among the SNPs involved in the PRS<sub>cross</sub> computation, top 10% SNPs (864) that contributed most to age by PRS<sub>cross</sub> on thickness of left IFC, right IFC and right posterior region of STG were respectively mapped to 259, 265, and 268 genes. For the left IFC, 212 among the 259 genes were expressed in the same cortical region, which were significantly over-representative over the 259 genes ( $p < 0.001$ ). These 212 genes formed four robust modules using WGCNA (Fig. 4a; Preservation Z-scores  $\geq 5.6$ ), namely, turquoise, blue, grey, and brown modules. Among the 4 modules, the turquoise module was the most robust module (Preservation Z-score = 15.0). Genetic Ontology (GO) analysis based on Fisher's exact test (FDR corrected) showed that the turquoise module largely reflected brain related biological processes, such as behavior, cognition, learning or memory and synaptic transmission (Fig. 4a). The major hub genes in this module included GRIN2A, CACNA1A, CTNND2, PLCO, PRKCB, and etc (Table 3). GO biological processes for the other three modules were less related to brain functions and did not survive for the FDR correction of multiple comparisons (Table S1 in the Supplementary Material).

Among the 265 genes, 226 were expressed in the right IFC, which were significantly over-representative over this full set of genes ( $p < 0.001$ ). Six modules were identified from these genes, including brown, turquoise, yellow, blue, green and grey (Fig. 4c; Preservation Z-scores  $\geq 1.5$ ) (Fig. 4c). Of the six modules, both brown and turquoise modules had the strongest Preservation Z-scores above 10. Brain-related biological processes were identified for both modules, i.e., positive regulation of axon extension involved in regeneration, neurogenesis, neuron projection development, dendrite development, and etc. But, none of these biological processes survived for the FDR correction

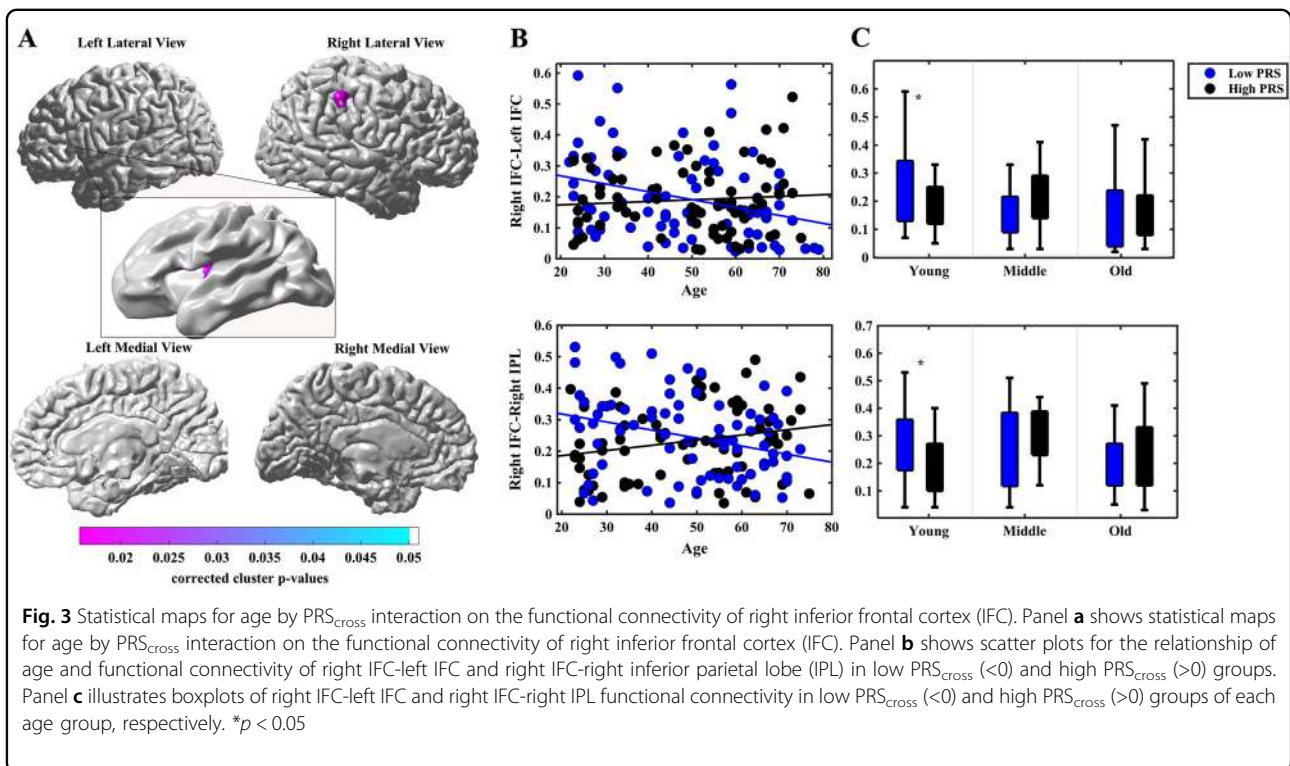
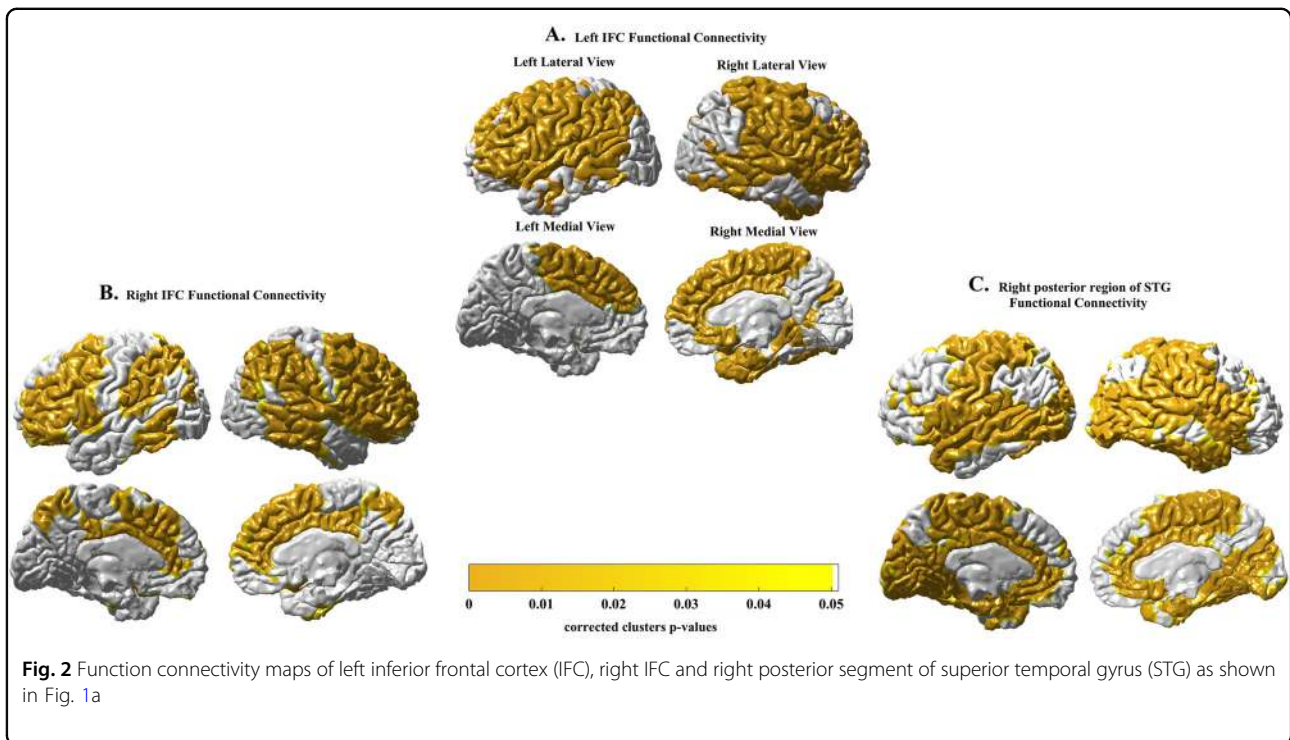
**Table 2** Age by PRS<sub>cross</sub> interaction on cortical thickness and functional connectivity

Brain regions	Age by PRS <sub>cross</sub>		Post hoc analysis association of age and brain regions		Slope Analysis  β (P-value)	Post hoc analysis in each age group  P-value
	Cluster size	P-value*	β (P-value)			
Cortical Thickness						
Left IFC	3382	<0.001	Low PRS <sub>cross</sub> group: −0.614 (<0.001) High PRS <sub>cross</sub> group: −0.106 (0.345)		−0.918 (0.001)	Young Adults: Low PRS <sub>cross</sub> > High PRS <sub>cross</sub> ; <i>p</i> = 0.031
						Middle-Aged Adults: Low PRS <sub>cross</sub> < High PRS <sub>cross</sub> ; <i>p</i> = 0.212
						Older Adults: Low PRS <sub>cross</sub> < High PRS <sub>cross</sub> ; <i>p</i> = 0.010
Right IFC	1175	0.035	Low PRS <sub>cross</sub> group: −0.436 (<0.001) High PRS <sub>cross</sub> group: 0.079 (0.481)		−0.867 (<0.001)	Young Adults: Low PRS <sub>cross</sub> > High PRS <sub>cross</sub> ; <i>p</i> = 0.017
						Middle-Aged Adults: Low PRS <sub>cross</sub> > High PRS <sub>cross</sub> ; <i>p</i> = 0.301
						Old Adults: Low PRS <sub>cross</sub> < High PRS <sub>cross</sub> ; <i>p</i> = 0.059
Right posterior segment of STG	2247	0.002	Low PRS <sub>cross</sub> group: −0.328 (0.003) High PRS <sub>cross</sub> group: −0.622 (<0.001)		−0.514 (0.032)	Young Adults: Low PRS <sub>cross</sub> > High PRS <sub>cross</sub> ; <i>p</i> = 0.051
						Middle-Aged Adults Low PRS <sub>cross</sub> > High PRS <sub>cross</sub> ; <i>p</i> = 0.060
						Old Adults: Low PRS <sub>cross</sub> < High PRS <sub>cross</sub> ; <i>p</i> = 0.043
Functional Connectivity						
Right IFC-Left-IFC	836	0.024	Low PRS <sub>cross</sub> group: −0.307 (0.004) High PRS <sub>cross</sub> group: 0.069 (0.537)		−0.688 (0.010)	Young Adults: Low PRS <sub>cross</sub> > High PRS <sub>cross</sub> ; <i>p</i> = 0.047
						Middle-Aged Adults: Low PRS <sub>cross</sub> < High PRS <sub>cross</sub> ; <i>p</i> = 0.105
						Old Adults: Low PRS <sub>cross</sub> > High PRS <sub>cross</sub> ; <i>p</i> = 0.652
Right IFC-Right IPL	1284	0.016	Low PRS <sub>cross</sub> group: −0.401 (<0.001) High PRS <sub>cross</sub> group: 0.095 (0.397)		−0.937 (<0.001)	Young Adults: Low PRS <sub>cross</sub> > High PRS <sub>cross</sub> ; <i>p</i> = 0.012
						Middle-Aged Adults: Low PRS <sub>cross</sub> > High PRS <sub>cross</sub> ; <i>p</i> = 0.644
						Old Adults: Low PRS <sub>cross</sub> < High PRS <sub>cross</sub> ; <i>p</i> = 0.425

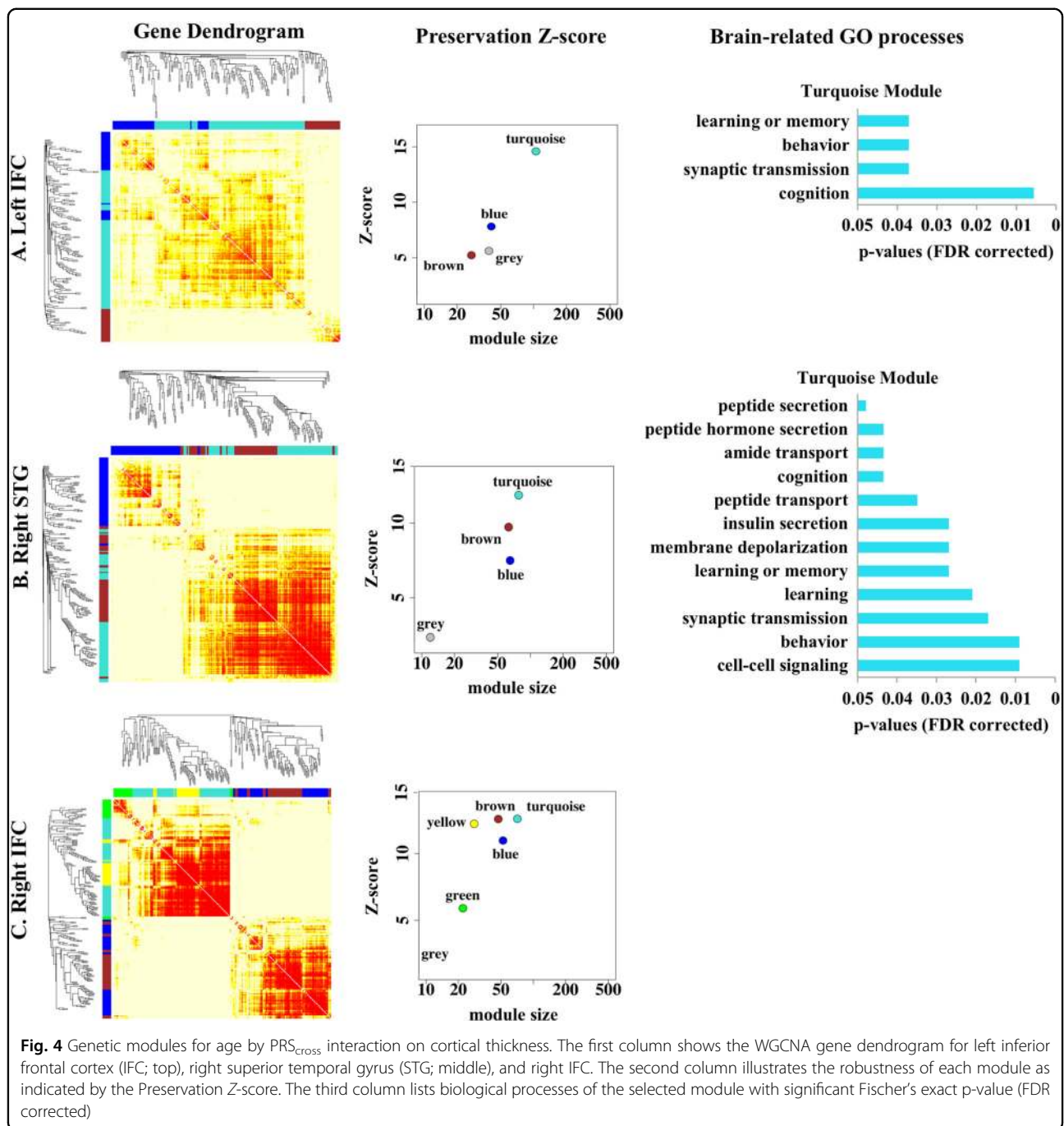
IFC inferior frontal cortex, STG superior temporal gyrus, IPL inferior parietal lobe

The columns respectively list brain regions with significant age by PRS<sub>cross</sub> interaction, clusters size and  $p$ -values,  $\beta$  and  $p$ -values for the associations of age and brain regions among low PRS<sub>cross</sub> (<0) and high PRS<sub>cross</sub> (>0) groups, slope analysis for comparing  $\beta$ -values between low and high PRS<sub>cross</sub> groups, and  $p$ -values for post hoc analysis in individual age groups

\*Corrected cluster  $p$ -value







of multiple comparisons. Likewise, GO biological processes for the other four modules also did not survive for the FDR correction of multiple comparisons (Table S2 in the Supplementary Material).

Similarly, among the 268 genes, 218 were expressed in the posterior region of STG, which was significantly over-representative over this full set of genes ( $p < 0.001$ ). Four modules were constructed from these genes (turquoise, brown, blue, grey in Fig. 4b; Preservation Z-scores  $\geq 2.3$ ) of which the turquoise module had the highest

Preservation Z-score of 12.0. This module largely reflected brain-related biological processes, such as behavior, cognition, learning or memory, synaptic transmission, and insulin secretion (Fig. 4b). Its major hub genes included GRIN2A, CACNA1A, CACNA1C, CTNND2, PLCO, PRKCB, ITPR1, and etc (Table 3). For the other three modules, GO biological processes identified were less related to brain functions and did not survive for the FDR correction of multiple comparisons (Table S3 in the Supplementary Material).

Table 3 Genetic modules and their biological processes most relevant to the brain function

Module	Preservation Z-score	Biological Processes	Genes
<b>Left Inferior Frontal Cortex Cortical Thickness</b>			
Turquoise	15.0	Behavior and Cognition	ADCY2 ATXN1 CACNA1A CACNB2 CADPS2 CTNND2 DACH1 GRID1 GRIN2A ITPR3 JAKMIP1 KCNJ4 LRRK2 NRG1 NTRK3 PAK7 PARK2 PCLO PRKAR1B PRKCB SORCS3 STX1B TUSC3
		behavior, cognition, learning or memory	
		Synaptic Transmission	
		synaptic transmission	
<b>Right Inferior Frontal Cortex Cortical Thickness</b>			
Turquoise	13.0	-	-
Yellow	12.0	-	-
<b>Right Superior Temporal Gyrus Cortical Thickness</b>			
Turquoise	25.0	Behavior and Cognition	ATXN1 CACNA1A CACNA1C CNTNAP2 CTNND2 GABBR2 GRIN2A ITPR1 KCNB1 KCNJ4 KIRREL3 NALCN NAV2 NLGN1 NTRK3 PCLO PRKAR1B PRKCB SORCS3 SYT13 THRB
		behavior, cognition, learning or memory	
		Synaptic Transmission	
		synaptic transmission	
		Metabolic Process	
		insulin secretion	
<b>Functional Connectivity between Right Inferior Frontal Cortex and Left Inferior Frontal Cortex</b>			
Turquoise	15.0	Behavior and Cognition	AAK1 ACSL6 ADCY8 AFF4 AFG3L2 AKTIP ALK ANK2 ANO2 ANTXR1 ANXA2 AQP9 ARHGEF3 ARNT ASH1L ASPH ATP2B2 ATXN1 BACH2 BAIAP2 BCL11B BTBD9 C11orf63 CA8 CACNA1D CACNA1I CACNG3 CADM2 CADPS CANT1 CASKIN1 CDC5L CDH2 CELSR1CHD9 CHERP CHL1 CHRNA3 CILP CMKLR1 CNGB3 CNIH3 CNKSR1 CNTN4 COBL COL19A1 CPT1A CRIM1 CTBP1 CTNNA2 CTSO CUX1 DACT2 DCC DDN DENND2A DGKI DGKZ DLC1 DLG2 DOCK4DOCK9 DPP6 DSCAM DSCAML1 DSP DYM EBF1 ELAVL2 ELMO1ERCC2 ERG FIG4 FOXN3 FOXO3 FRMD6 GABBR2 GABRG3 GFRA1 GNAL GPD2 GRIN2A GRM5 HECW1 HYOU1 IFIT1 IGF1R IL1RAP INPP5B ITGA9 ITSN2 JARID2 JPH4 KCND3 KCNP4 KCNMA1 KCNQ3 KCNQ5 KCTD8 KDM3B KLF12 KLHL1 KRTAP5-9 KSR2 LDB2 LGI1 LMO2 LMTK2 LPCAT1 LPHN3 LRP8 LRRC4C LRRC8A LRRIP1 LRRK2 LRRN1 LSAMP MACROD2 MAP2K4 MAP4K3 MARK3 MASTL MCTP1 MED12L MIB1 MMP17
		Behavior, cognition, learning or memory, locomotion	
		Synaptic Transmission and Synaptogenesis	
		Synaptic transmission, GABAergic synaptic transmission, glutamatergic synaptic transmission, glutamate receptor signaling pathway, cell surface receptor signaling pathway, transmembrane receptor protein tyrosine kinase signaling pathway, enzyme linked receptor protein signaling pathway, regulation of synaptic plasticity, neurotransmitter transport, regulation of transmembrane transporter activity, ion transmembrane transport, calcium ion transmembrane transport, regulation of small GTPase mediated signal transduction, regulation of alpha-amino-3-hydroxy-5-methyl-4-isoxazolepropionate (AMPA) selective glutamate receptor activity, N-methyl-D-aspartate	

Table 3 continued

Module	Preservation Z-score	Biological Processes	Genes
		(NMDA) receptor clustering, protein localization to synapse, cellular response to catecholamine, regulation of excitatory postsynaptic membrane potential	MINAT1 MOC52 MYH9 MYRIP NCAN NLGN1 NOS1 NPAS2 NPR3 NRG3 NRXN1 NUAK1NUMB OXR1 PACRG PARK2 PBX3 PCLO PDE10A PDE4D PDE7B PDZD8 PEX5L PHACTR1 PHACTR2 PIK3R1 PKD1L1 PLCB1 PLXNA4 PPP2R2B PRKAA1 PRKCE PRKG2 PTPRD PTPRE PTPRG PTPRJ PTPRN2 PTPRR PTPRT PYDN RAB31 RAPGEF4 RASA2 RBL2 RBMS3 RCAN1 RELN RFTN1 RNF168 ROBO2 RORA RPRD1A RPS6KA2 RTN4RL1 RYR2 SCOCSEMA5A SH3GL2 SIM2 SIPA1L2 SKAP1 SLC1A1 SLC22A3 SLC37A3 SLC6A1 SLC8A1 SLIT2 SMG6 SMOC2 SNTG1 SNX25 SOD2 SORCS1 SORCS3 SOX5 STAM STARD13 STAT4 STAT6 STK17A STYXL1 SV2B SYN3 SYNE1 TAF3 TBC1D13 TBC1D4TBC1D8 TFB2M THRB TIAM1 TNIK TRIM8 TTC8 TTN TTYH3 TUSC3 VAV3 VAX2 VEGFA VGLL4 VPS13A VWC2L XPR1 ZBTB46 ZC3H14 ZFPW2 ZMYM4 ZNF101 ZNF165 ZNF18 ZNF317 ZNF423 ZNF461 ZNF516 ZNF580 ZNF77 ZNF862 ZNF883
		Brain Development and Organization	
		Nervous system development, central nervous system development, anatomical structure development, brain development, neurogenesis, synapse organization, neuron differentiation, cell morphogenesis involved in neuron differentiation, stimulus neuron projection development, axonogenesis, axon guidance, dendrite development, axon extension involved in axon guidance	
		Metabolic Process	
		Regulation of metabolic process, phosphate-containing compound metabolic process, insulin-like growth factor receptor signaling pathway	
Functional Connectivity between Right Inferior Frontal Cortex and Inferior Parietal Lobe			
Turquoise	31.0	Behavior and Cognition	AAK1 ACSL6 ADAMTS16 ADCY9 ADIPOQ AFF4 ANK3 APP ARHGAP26 ARHGEF3 ASPH ATP2B2 ATP8A2 BCL11B BCL2L14 BTBD9 CA10 CACNA1D CACNA2D1 CACNB2 CADM2 CADPS CDC42BPA CDH13 CDH22 CHERP CHST11 CNR1 CNTN4 CNTN5 CNTNAP2 CRIM1 CRISPLD2 CTNNA2 DGKI DSP1 DLC1 DOCK3 DOCK4 DPPA2 DPP6 DSCAML1 EGFR EGLN1 EPB41L3 ERBB4 EVC EYA1 EYS FBXO11 FGF14 FMN2 FOXJ2 FOXP2 GABRG2 GABRG3 GCG GJB6 GNAL GPR55 GREM2 GRHL2 GRIN2A GRIP2 GRM1 HCN1 HDAC9 HMG2 IGF1R IL1RN ITGA9 ITPR1 ITSN1 ITSN2 KALRN KCNA6 KCNAB1 KCNQ5 KCTD16 KIF20B KIF26B KIF5C KIRREL3 KRAS LMTK2 LPCAT1 LRP8 LRRK16A LRRK2 LYST MACF1 MAGI2 MAP2K4 MAPK14 MFG8 MIDN MNAT1 MTOR MURC MYO10 NEGR1 NELL1 NLGN1 NOS1AP NRXN1 OLFM3 OPCML OSBPL8 PBX1 PCDH15 PDE10A PDE4D PDE8B

### Biological processes for age by gene interaction on functional connectivity

Top 10% SNPs that most contributed to age by  $PRS_{cross}$  on the functional connectivity of the right IFC-left IFC (7638) and the functional connectivity of the right IFC-right IPL (5435) were mapped to 1871 genes and 1417, respectively.

Assuming that genes with common expression profiles between two cortical regions underlie the molecular basis for the functional organization. Genes with similar expression patterns between right IFC and left IFC as well as between right IFC and right IPL were identified via maxT, Kolmogorov–Smirnov test (KS test) and Radial Kolmogorov–Smirnov test (RKStest) analyses. Gene expression profiles of these regions were obtained from the Allen Brain Atlas gene transcriptome data. For the functional connectivity of right IFC-left IFC, 1505 out of 1871 genes were commonly expressed in both left and right IFC. Nevertheless, maxT, KStest and RKStest analyses only revealed 1078 genes expressed in bilateral IFC at the same level of gene expression and its variance ( $p > 0.05$ ). These 1078 genes were significantly over-representative over this full set of genes ( $p < 0.001$ ). Five genetic modules were further identified using WGCNA (Fig. 5a, Preservation Z-scores  $\geq 12.0$ ), namely, blue, turquoise, brown, yellow, and grey modules. Of note, genetic network structures among these genes were much more robust than those seen in Fig. 4 with turquoise module showing a strong Preservation Z-score of 25.0. This module largely reflected brain-related biological processes such as behavior, cognition, learning or memory, brain development, neuron projection development, synaptic transmission, GABAergic synaptic transmission, glutamate receptor signaling pathway, insulin-like growth factor receptor signaling pathway, regulation of synaptic plasticity and synapse organization (significant FDR corrected p-values reported in Table S4 of the Supplementary Material). The major hub genes of this module comprised GRIN2A, GRM5, CTNND2, CACNA1D, PLCO, PRKCE, ROBO2, SLIT2, RELN, GABRG2, SLC6A1, IGF1R, and etc (Table 3). For the other 4 modules, GO biological processes were less related to brain and none of them survived for the FDR correction of multiple comparisons (Table S4 in the Supplementary Material).

Likewise, for the functional connectivity of the right IFC-right IPL, 1150 out of 1417 genes were commonly expressed in both right IFC and right IPL. However, only 901 genes were not differentially expressed in the right IFC and right IPL ( $p > 0.05$ ), which was significantly over-representative over this full set of genes ( $p = 0.0035$ ). These 901 genes formed six modules using WGCNA, including turquoise, green, brown, blue, yellow and grey modules (Preservation Z-scores  $\geq 10.0$ ; Fig. 5b). Among

the six modules, the turquoise module had strongest Preservation Z-scores of 31.0 and was most reflective of brain-related biological processes, such as cognition, learning or memory, nervous system development, neuron projection development, brain development, synaptic transmission, GABAergic synaptic transmission, regulation of glutamatergic synaptic transmission, synapse organization and neurotrophin signaling pathway (significant FDR corrected p-values reported in Table S5 of the Supplementary Material). The major hub genes of this module comprised of GRIN2A, GRM5, CTNND2, CACNA1D, PRKCB, ROBO2, SLIT2, GABRG2, SLC6A1, APP, and etc (Table 3). The blue and green modules with Preservation Z-scores of 17.0 and 19.0 respectively also showed significant biological processes after the FDR correction for multiple comparisons. However, most of the biological processes associated with these two modules were non-brain related (significant FDR corrected p-values reported in Table S5 of the Supplementary Material). GO biological processes of the other three modules were also less related to the brain and did not survive for the FDR correction of multiple comparisons (Table S5 in the Supplementary Material).

### Discussion

This study examined whether the polygenic risk for psychiatric disorders modulated age-related alterations in cortical thickness and its corresponding functional connectivity using a Chinese sample comprised of adults aged from 21 years and above. Our results showed age-related cortical thinning in bilateral IFC and STG and alterations in the functional connectivity between bilateral IFC and between right IFC and right IPL as a function of the polygenic risk for psychiatric disorders. The genes, that were involved in this polygenic risk and contributed most to age-related alterations in cortical thickness and functional connectivity, were expressed in the corresponding cortical regions and had biological processes related to neural plasticity, synaptogenesis and metabolism. Especially, genes identified through the genotype-functional connectivity association analysis were commonly expressed in both cortical regions and formed strong gene networks contributing to neural plasticity, synaptogenesis, and metabolism, suggesting convergent evidence on potential candidate molecular mechanisms for aging brain.

Our findings underlined a modulative role of psychiatric risk genes in aging brain, particularly in cortical regions that have been considered as hallmarks of normal aging and psychiatric disorders. The IFC and STG show pronounced age-related cortical thinning<sup>11,12,51</sup>. Likewise, individuals with psychiatric disorders, such as schizophrenia and bipolar disorders, show cortical thinning in these brain regions as compared to healthy adults<sup>52–56</sup>. In



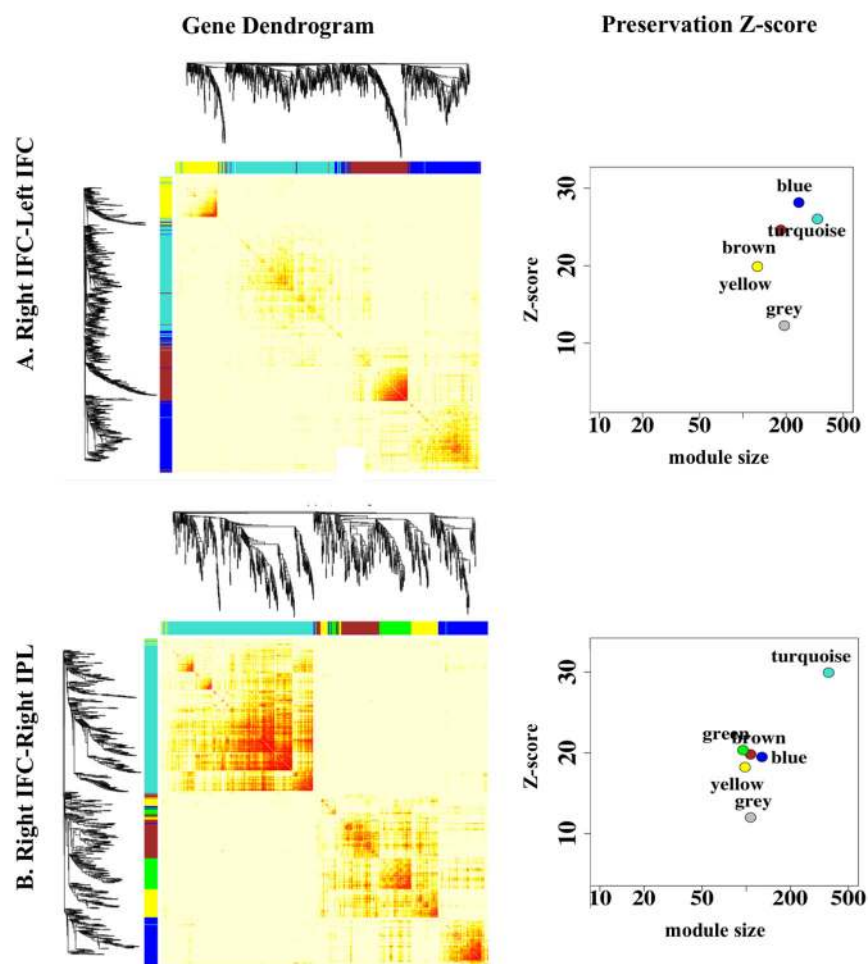


**Fig. 5** Genetic modules. The first column shows the WGCNA gene dendrogram for shared genes between bilateral inferior frontal cortex (IFC; top) and between IFC and right inferior parietal lobe (IPL; bottom). The second column illustrates the robustness of each module as indicated by the Preservation Z-score

parallel with brain morphology, functional connectivity between bilateral IFC and between right IFC and IPL are also found to be susceptible to both normal aging and psychiatric disorders<sup>14,15,57</sup>. Taken together, these findings suggest that brain morphology and functional organization commonly vulnerable to aging and psychiatric disorders are as a function of the polygenic risk for psychiatric disorders.

Our findings suggested antagonistic pleiotropy, that is, impact of certain genes may differ at different stages of life. By far, this phenomenon has been substantially supported by the findings of APOE and COMT on behavioral and neural endophenotypes across lifespan<sup>25,58–64</sup>. Apparently, this phenomenon was also supported by our findings related to the polygenic variants for psychiatric disorders. Neural benefits that are genetically programmed by polygenic risk genes for psychiatric disorders include thicker cortex and stronger functional

connectivity in early life but with a potential bearing towards neural susceptibility in late life. Nevertheless, our findings showed that older adults with a lower polygenic risk was associated with greater age-related cortical thinning and reduction in the functional connectivity as compared to those with a higher polygenic risk. This is opposite to what is shown in Caucasian populations<sup>65,66</sup>, which underscores the importance of population differences in genetic influences on imaging phenotypes.

This study showed shared biological processes contributing to age-related cortical thinning in bilateral IFC and right STG and reduction in their functional connectivity. These processes involve biological functions related to behaviors, cognition, learning and memory, synaptic transmission, and metabolism. These biological functions may highlight potential molecular mechanisms for understanding the role of IFC morphology and functional organization in an age-related decline in memory

and learning<sup>67,68</sup>. First, this study highlighted a set of genes (GRIN2A, CACNA1A, CACNA1C, CTNND2, PLCO, PRKC, GRM1, GRM5, etc.). These genes implicated long-term potentiation (LTP) as one of their major functions. LTP is a form of activity-dependent plasticity that results in a persistent enhancement of synaptic transmission<sup>69</sup>. LTP requires coincident detection of pre- and post-synaptic depolarization, which is accomplished through the NMDA receptor, a voltage-dependent subtype of glutamate receptor that allows permeation of calcium and other cations. In addition, there exist a wide range of other forms of LTP that is induced through activation of the metabotropic glutamate receptor<sup>70</sup>. Indeed, experimentally removing or altering certain genes in mice, such as CACNA1C, GRIN2A and GRM5, modifies LTP, which results in a long-lasting increase in the strength of synaptic transmission<sup>71–74</sup>. Even though these molecular mechanisms of LTP were initially discovered in the hippocampus, they exist at these synapses and throughout the brain. It has been demonstrated that LTP-related changes in synaptic strength occur as memory is formed at various sets of synapses in the brain<sup>75</sup>. LTP-synaptic plasticity in the prefrontal cortex is modified due to aging<sup>76–78</sup>. Acetylcholine, one of major available pharmaceutical treatments for Alzheimer's disease, targets to improve memory function via enhancing the effects of LTP induction<sup>79</sup>. Complementary to animal and drug research mentioned above, this study employed brain imaging and bioinformatics techniques and provided new evidence on a potential fundamental molecular mechanism of LTP in age-related alterations in IFC thickness and its functional organization.

Second, this study also identified a set of genes (IGF1R, PIK3R1, PLCB1, ITPR1, CACNA1C, etc), with insulin secretion and insulin-like growth factor signaling functions, in link with age-related cortical thinning of the temporal cortex and reduction in the functional connectivity of the prefrontal cortex. There have been great efforts to link the brain insulin/IGF1 with neuropathologies mainly because canonical signaling of their receptors, including the phosphoinositide 3-kinase (PI3K)–AKT–forkhead box protein O (FOXO) and RAS–mitogen-activated protein kinase (MAPK) pathways, influences apoptosis, neuronal antioxidant defence, tau phosphorylation, neuronal survival, and synaptic transmission<sup>80,81</sup>. Insulin seems to protect against the toxic effects of  $\alpha$ -amino-3-hydroxy-5-methyl-4-isoxazolepropionic acid receptor (AMPA), oxygen/glucose deprivation and to prevent apoptosis<sup>82</sup>. Losing the protective effects of insulin, the brain may be at an increased risk for neurodegeneration. IGF1 is also suggested to play a beneficial role in neurodegenerative processes (1) by its potent pro-survival effects on damaged neurons through the PI3K-ATK pathway<sup>83</sup>; (2) by promoting amyloid clearance

through blood-brain-barrier for the protection against Alzheimer's pathology<sup>84</sup>; and (3) by blocking the action of inflammatory cytokines for protecting neurons against maladaptive inflammation that is a common process underlying in neurodegeneration<sup>85</sup>. Moreover, both insulin and IGF1 influence learning and memory by modulating neuronal plasticity. They modulate LTP, long-term depression, and changes in synaptic strength by changing transmission and synthesis of glutamate and GABA receptors through the PI3K-ATK pathway and modulate neuronal excitability by affecting ion-channels through MAPK pathways<sup>83</sup>. Disruptions of IGR1R and CACNA1C in animal models are associated with enhanced apoptosis, reduced neuronal survival rate, and lower glucose metabolism<sup>80,86,87</sup>. Intriguingly, glutamate or amyloid peptides interfere with IGF1R signaling, leading to a state of IGF1 resistance in Alzheimer's disease, a trait that may profoundly affect its course<sup>84</sup>. Clinical trials with insulin show improved cognition in patients with Alzheimer's disease<sup>88</sup>. Although it is unclear why the metabolic functions only targeted to aged-related brain atrophy in the temporal cortex and functional disconnection in the frontal cortex shown in this study, the spatial distribution of the insulin and IGF1 in the brain are highly dependent on the availability of glucose and lipids to brain centers involved in energy allocation. Substantial evidence from FDG-PET/fMRI-studies suggests an association between glucose consumption and functional connectivity in the frontal region<sup>89,90</sup>. The rest-state glucose consumption is remarkably correlated with the distribution of amyloid plaques<sup>91</sup>. Moreover, dysregulation of glucose metabolism, such as hypoglycemia, has been found to be associated with thinning of the superior temporal and prefrontal cortex<sup>92,93</sup>. Notwithstanding, hypoglycemia is also associated with decreased prefrontal functional connectivity within the default-mode network and frontal-parietal network<sup>94,95</sup>. These findings highlight possible “metabolism hypothesis” for aging and Alzheimer's disease.

The most intriguing finding in this study demonstrated that the genes contributing to age-related alterations in the frontal functional connectivity formed much more robust gene networks (all Preservation Z-score > 10) than those observed in cortical morphology, supporting the idea on common molecular bases for age-related alterations in the functional communication between two brain regions. These molecular functions included synaptic transmission, neurotrophin signaling pathway, synaptogenesis, and metabolism. Again, the genes (GRIN2A, GRM1, PLCO, IGF1R, PIK3R1, PLCB1, etc), identified based on the frontal functional connectivity, largely overlapped with those derived from the frontal cortical morphology. As mentioned earlier, they are involved in the glutamatergic and GABAergic transmission and

metabolic processes that regulate neural plasticity important for learning and memory<sup>83</sup>. Indeed, reduced GABAergic signaling is associated with less IFC engagement during learning task<sup>96</sup>. Age-related dysregulation of GABAergic signaling in IFC contributes to working memory impairment in aging<sup>97</sup>. Decline in glutamate neurotransmitter is associated with dysregulated synaptic plasticity and impaired working memory<sup>98</sup>. Likewise, the neurotrophin signaling pathway, comprised of MAPK14, PIK3R1, FOXO3, ITPR1, VAV3, EGFR, ERBB4, PRKCE, ADCY9, KRAS, and etc, involves a family of trophic factors that contribute to differentiation and survival of neural cells. The neurotrophin signaling is regulated by connecting a variety of intracellular signaling cascades, which include MAPK pathway, PI3K-pathway, and PLC pathway, and transmits positive signals to enhance neural survival and growth. Hence, this signal plays an important role for neural development, neuroprotection against age-related cellular insults, neural plasticity, and higher-order activities such as learning and memory<sup>99,100</sup>. Decreases in the expression of MAPK, neurotrophin and their receptors are associated with advanced aging<sup>101–103</sup>. Most importantly, neural metabolism, synaptic transmission, neurotrophin are all critical for synaptogenesis. This study showed that genes (VAV3, ROBO2, SLIT2, RELN, IGF1R, CACNA1D, CACNA1I, etc) involve in numerous biological processes, including dendrite development, axonogenesis, and neuron projection, closely associated with synaptogenesis. The establishment of precise connections among neurons usually requires a balance between excitatory and inhibitory synapses. Both glutamatergic and GABAergic transmission mediate dendritic growth, arbor and length during synaptogenesis<sup>104,105</sup>, which shapes the cortical circuitry during brain development<sup>105,106</sup>. Likewise, neurotrophin factors regulate several functions for synapse formation, including enhancement of transmitter release and increased concentration of vesicles. Furthermore, both insulin and IGF1 regulate dendritogenesis, synapse maintenance, and axon guidance through PI3K-AKT signaling<sup>107</sup>. IGF1 involves in the production and migration of GABAergic and glutamatergic neurons and thus contributes to the formation of appropriate circuitries in the cortex<sup>108</sup>. All together support the idea on age-related reduction in capacity of synaptogenesis<sup>109</sup>.

This study is best considered as preliminary and exploratory and intended to provide a strategy for the analysis of gene-age interdependence and identify candidate biological processes that might mediate the influence of aging associated with the genetic risk for psychiatric disorders on neurodegeneration. While combining genotype and transcriptome data with multi-modal brain images is highly unique, it is nevertheless a modest sample size for genomic analyses. However, our findings do suggest biologically plausible candidate processes for age-

related degeneration in both brain morphology and functional organization. Especially, genes modulating the age-related functional dysconnectivity are well expressed in the functionally connected brain regions and form strong genetic networks contributing to synaptic transmission and synaptogenesis.

In conclusion, this preliminary study suggests the feasibility to identify biological mechanisms for aging brain via integrating genotype and transcriptome with neuro-image data. Our findings suggest that neural plasticity and synaptogenesis, particularly regulated by glutamatergic and GABAergic transmission, neurotrophin signaling, and neural metabolism, are core biological mechanisms contributing to age-related cortical thinning and functional disconnection.

#### Acknowledgements

This research is supported by the National Medical Research Council (NMRC; NMRC/CBRG/0039/2013).

#### Author details

<sup>1</sup>Department of Biomedical Engineering, National University of Singapore, Singapore 117576, Singapore. <sup>2</sup>Singapore Institute for Clinical Sciences, The Agency for Science, Technology and Research, Singapore 117609, Singapore. <sup>3</sup>Clinical Imaging Research Center, National University of Singapore, Singapore 117456, Singapore

#### Competing interests

The authors declare that they have no competing financial interests.

**Publisher's note:** Springer Nature remains neutral with regard to jurisdictional claims in published maps and institutional affiliations.

#### Supplementary information

The online version of this article (<https://doi.org/10.1038/s41398-017-0036-z>) contains supplementary material.

Received: 7 June 2017 Revised: 4 August 2017 Accepted: 7 September 2017  
Published online: 11 December 2017

#### References

- Grieve, S. M., Korgaonkar, M. S., Koslow, S. H., Gordon, E. & Williams, L. M. Widespread reductions in gray matter volume in depression. *NeuroImage Clin* **3**, 332–339 (2013).
- Kong, L. et al. Reduced gray to white matter tissue intensity contrast in schizophrenia. *PLoS ONE* **7**, e37016 (2012).
- Kuperberg, G. R. et al. Regionally localized thinning of the cerebral cortex in schizophrenia. *Arch. Gen. Psychiatr.* **60**, 878–888 (2003).
- Lan, M. J. et al. Cortical thickness differences between bipolar depression and major depressive disorder. *Bipolar. Disord.* **16**, 378–388 (2014).
- Selvaraj, S. et al. Grey matter differences in bipolar disorder: a meta-analysis of voxel-based morphometry studies. *Bipolar. Disord.* **14**, 135–145 (2012).
- Tu, P. C. et al. Regional cortical thinning in patients with major depressive disorder: a surface-based morphometry study. *Psychiatr. Res.* **202**, 206–213 (2012).
- Fjell, A. M. et al. High consistency of regional cortical thinning in aging across multiple samples. *Cereb. Cortex* **19**, 2001–2012 (2009).
- Raz, N. Aging of the brain and its impact on cognitive performance: Integration of structural and functional findings. In: Salthouse FIMCTA (ed). *The handbook of aging and cognition* (2nd ed.). Lawrence Erlbaum Associates Publishers: 2000, pp 1–90.

9. Raz, N., Rodrigue, K. M., Head, D., Kennedy, K. M. & Acker, J. D. Differential aging of the medial temporal lobe: a study of a five-year change. *Neurology*. **62**, 433–438 (2004).
10. Ziegler, G. et al. Brain structural trajectories over the adult lifespan. *Hum. Brain Mapp.* **33**, 2377–2389 (2012).
11. Salat, D. H. et al. Thinning of the cerebral cortex in aging. *Cereb. Cortex*. **14**, 721–730 (2004).
12. Lemaitre, H. et al. Normal age-related brain morphometric changes: non-uniformity across cortical thickness, surface area and gray matter volume? *Neurobiol. Aging*. **33**, 617.e611–619 (2012).
13. van den Heuvel, M. P. & Hulshoff Pol, H. E. Exploring the brain network: a review on resting-state fMRI functional connectivity. *European Neuropsychopharmacol.* **20**, 519–534 (2010).
14. Barkhof, F., Haller, S. & Rombouts, S. A. Resting-state functional MR imaging: a new window to the brain. *Radiology*. **272**, 29–49 (2014).
15. Sala-Llonch, R., Bartres-Faz, D. & Junque, C. Reorganization of brain networks in aging: a review of functional connectivity studies. *Front Psychol*. **6**, 663 (2015).
16. Baker, J. T. et al. Disruption of cortical association networks in schizophrenia and psychotic bipolar disorder. *JAMA Psychiatr*. **71**, 109–118 (2014).
17. Menon, V. Large-scale brain networks and psychopathology: a unifying triple network model. *Trends Cogn. Sci.* **15**, 483–506 (2011).
18. Meyer-Lindenberg, A. et al. Evidence for abnormal cortical functional connectivity during working memory in schizophrenia. *Am. J. Psychiatr.* **158**, 1809–1817 (2001).
19. Crossley, N. A. et al. The hubs of the human connectome are generally implicated in the anatomy of brain disorders. *Brain*. **137**(Pt 8), 2382–2395 (2014).
20. Goodkind, M. et al. Identification of a common neurobiological substrate for mental illness. *JAMA Psychiatr*. **72**, 305–315 (2015).
21. Hashimoto, R. et al. Imaging genetics and psychiatric disorders. *Curr. Mol. Med.* **15**, 168–175 (2015).
22. Stein, J. L. et al. Voxelwise genome-wide association study (vGWAS). *Neuroimage*. **53**, 1160–1174 (2010).
23. Bonora, E. et al. Maternally inherited genetic variants of CADPS2 are present in autism spectrum disorders and intellectual disability patients. *EMBO Mol Med*. **6**, 795–809 (2014).
24. Havik, B. et al. The complement control-related genes CSMD1 and CSMD2 associate to schizophrenia. *Biol. Psychiatr.* **70**, 35–42 (2011).
25. Lee, A. & Qiu, A. Modulative effects of COMT haplotype on age-related associations with brain morphology. *Hum. Brain Mapp.* **37**, 2068–2082 (2016).
26. Hodgkinson, C. A. et al. Disrupted in schizophrenia 1 (DISC1): association with schizophrenia, schizoaffective disorder, and bipolar disorder. *Am. J. Hum. Genet.* **75**, 862–872 (2004).
27. Li, M. L. et al. Morphological changes in gray matter volume correlate with catechol-O-methyl transferase gene Val158Met polymorphism in first-episode treatment-naïve patients with schizophrenia. *Neurosci. Bull.* **31**, 31–42 (2015).
28. Szeszko, P. R. et al. DISC1 is associated with prefrontal cortical gray matter and positive symptoms in schizophrenia. *Biol. Psychol.* **79**, 103–110 (2008).
29. Takahashi, T. et al. The Disrupted-in-Schizophrenia-1 Ser704Cys polymorphism and brain morphology in schizophrenia. *Psychiatr. Res.* **172**, 128–135 (2009).
30. Tian, T. et al. Catechol-O-methyltransferase Val158Met polymorphism modulates gray matter volume and functional connectivity of the default mode network. *PLoS ONE*. **8**, e78697 (2013).
31. Escott-Price, V. et al. Common polygenic variation enhances risk prediction for Alzheimer's disease. *Brain*. **138**, 3673–3684 (2015).
32. Gratten, J., Wray, N. R., Keller, M. C. & Visscher, P. M. Large-scale genomics unveils the genetic architecture of psychiatric disorders. *Nat. Neurosci.* **17**, 782–790 (2014).
33. Lubke, G. H. et al. Estimating the genetic variance of major depressive disorder due to all single nucleotide polymorphisms. *Biol. Psychiatr.* **72**, 707–709 (2012).
34. Ripke, S. et al. Identification of risk loci with shared effects on five major psychiatric disorders: a genome-wide analysis. *Lancet*. **381**, 1371–1379 (2013).
35. Sibille, E. Molecular aging of the brain, neuroplasticity, and vulnerability to depression and other brain-related disorders. *Dialogues. Clin. Neurosci.* **15**, 53–65 (2013).
36. Krienen, F. M., Yeo, B. T., Ge, T., Buckner, R. L. & Sherwood, C. C. Transcriptional profiles of supragranular-enriched genes associate with corticocortical network architecture in the human brain. *Proc Natl Acad Sci U S A*. **113**, E469–478 (2016).
37. Richiardi, J. et al. BRAIN NETWORKS. Correlated gene expression supports synchronous activity in brain networks. *Science*. **348**, 1241–1244 (2015).
38. Hawrylycz, M. J. et al. An anatomically comprehensive atlas of the adult human brain transcriptome. *Nature*. **489**, 391–399 (2012).
39. Langfelder, P. & Horvath, S. WGCNA: an R package for weighted correlation network analysis. *BMC Bioinform.* **9**, 559 (2008).
40. Murray, L. J. & Ranganath, C. The dorsolateral prefrontal cortex contributes to successful relational memory encoding. *J Neurosci*. **27**, 5515–5522 (2007).
41. Fischl, B. et al. Whole Brain Segmentation: Automated Labeling of Neuroanatomical Structures in the Human Brain. *Neuron*. **33**, 341–355 (2002).
42. Fischl, B. & Dale, A. M. Measuring the thickness of the human cerebral cortex from magnetic resonance images. *Proc Natl Acad Sci U S A*. **97**, 11050–11055 (2000).
43. Zhong, J. & Qiu, A. Multi-manifold diffeomorphic metric mapping for aligning cortical hemispheric surfaces. *Neuroimage*. **49**, 355–365 (2010).
44. Jiang, L., Willner, D., Danoy, P., Xu, H. & Brown, M. A. Comparison of the performance of two commercial genome-wide association study genotyping platforms in Han Chinese samples. *G3*. **3**, 23–29 (2013).
45. Oliphant, A., Barker, D. L., Stuelplnagel, J. R. & Chee, M. S. BeadArray technology: enabling an accurate, cost-effective approach to high-throughput genotyping. *Biotechniques*. **Suppl: 56-58**, 60–51 (2002).
46. Cross-Disorder Group of the Psychiatric Genomics Consortium. Identification of risk loci with shared effects on five major psychiatric disorders: a genome-wide analysis. *Lancet*. **381**, 1371–1379 (2013).
47. Chung, M. K., Worsley, K. J., Nacewicz, B. M., Dalton, K. M. & Davidson, R. J. General multivariate linear modeling of surface shapes using SurfStat. *Neuroimage*. **53**, 491–505 (2010).
48. Pollard KS, Dudoit S, van der Laan MJ. Multiple testing procedures: the multtest package and applications to genomics. *Bioinformatics and computational biology solutions using R and bioconductor*. Springer 2005, pp 249–271.
49. Rahmatallah, Y., Emmert-Streib, F. & Glazko, G. Gene Sets Net Correlations Analysis (GSNCA): a multivariate differential coexpression test for gene sets. *Bioinformatics*. **30**, 360–368 (2014).
50. Rahmatallah Y, Glazko G. Gene Set Analysis in R—the GSAR Package.
51. Crivello, F., Tzourio-Mazoyer, N., Tzourio, C. & Mazoyer, B. Longitudinal assessment of global and regional rate of grey matter atrophy in 1,172 healthy older adults: modulation by sex and age. *PLoS ONE*. **9**, e114478 (2014).
52. Gong, Q. et al. A neuroanatomical signature for schizophrenia across different ethnic groups. *Schizophr. Bull.* **41**, 1266–1275 (2015).
53. Hajek, T. et al. Brain structural signature of familial predisposition for bipolar disorder: replicable evidence for involvement of the right inferior frontal gyrus. *Biol. Psychiatr.* **73**, 144–152 (2013).
54. Makris, N. et al. Cortical thinning of the attention and executive function networks in adults with attention-deficit/hyperactivity disorder. *Cereb. Cortex*. **17**, 1364–1375 (2007).
55. Rimol, L. M. et al. Cortical thickness and subcortical volumes in schizophrenia and bipolar disorder. *Biol psychiatr*. **68**, 41–50 (2010).
56. Schiffer, B. et al. Impulsivity-related brain volume deficits in schizophrenia-addiction comorbidity. *Brain*. **133**, 3093–3103 (2010).
57. Stephan, K. E., Friston, K. J. & Frith, C. D. Dysfunction in Schizophrenia: From Abnormal Synaptic Plasticity to Failures of Self-monitoring. *Schizophr. Bull.* **35**, 509–527 (2009).
58. Borghesani, P. R. et al. Altered medial temporal lobe responses during visuospatial encoding in healthy APOE\*4 carriers. *Neurobiol. Aging*. **29**, 981–991 (2008).
59. Dennis, N. A. et al. Temporal lobe functional activity and connectivity in young adult APOE varepsilon4 carriers. *Alzheimer's Dementia*. **6**, 303–311 (2010).
60. Filbey, F. M., Chen, G., Sunderland, T. & Cohen, R. M. Failing compensatory mechanisms during working memory in older apolipoprotein E-epsilon4 healthy adults. *Brain. Imaging. Behav.* **4**, 177–188 (2010).
61. Hayden, K. M. et al. Effects of family history and apolipoprotein E epsilon4 status on cognitive decline in the absence of Alzheimer dementia: the Cache County Study. *Arch. Neurol.* **66**, 1378–1383 (2009).



62. Jochemsen, H. M., Muller, M., van der Graaf, Y. & Geerlings, M. I. APOE epsilon4 differentially influences change in memory performance depending on age. The SMART-MR study. *Neurobiol. Aging*. **33**, 832.e815–822 (2012).
63. Lind, J. et al. Reduced functional brain activity response in cognitively intact apolipoprotein E epsilon4 carriers. *Brain* **129**, 1240–1248 (2006).
64. Xu, G. et al. The influence of parental history of Alzheimer's disease and apolipoprotein E epsilon4 on the BOLD signal during recognition memory. *Brain* **132**, 383–391 (2009).
65. Kauppi, K. et al. Polygenic risk for schizophrenia associated with working memory-related prefrontal brain activation in patients with schizophrenia and healthy controls. *Schizophr. Bull.* **41**, 736–743 (2015).
66. Walton, E. et al. Prefrontal inefficiency is associated with polygenic risk for schizophrenia. *Schizophr. Bull.* **40**, 1263–1271 (2014).
67. Malonebeach, E. E. & Zarit, S. H. Current research issues in caregiving to the elderly. *Int. J. Aging. Hum. Dev.* **32**, 103–114 (1991).
68. Tasman A., Kay J., Lieberman J. A., First M. B., Riba M. *Psychiatry, 2 Volume Set*. Wiley 2015.
69. Lynch, M. A. Long-term potentiation and memory. *Physiol. Rev.* **84**, 87–136 (2004).
70. Huber, K. M., Kayser, M. S. & Bear, M. F. Role for rapid dendritic protein synthesis in hippocampal mGluR-dependent long-term depression. *Science* **288**, 1254–1257 (2000).
71. Kiyama, Y. et al. Increased thresholds for long-term potentiation and contextual learning in mice lacking the NMDA-type glutamate receptor epsilon1 subunit. *J. Neurosci* **18**, 6704–6712 (1998).
72. Moosmang, S. et al. Role of hippocampal Cav1.2 Ca<sup>2+</sup> channels in NMDA receptor-independent synaptic plasticity and spatial memory. *J. Neurosci* **25**, 9883–9892 (2005).
73. Sakimura, K. et al. Reduced hippocampal LTP and spatial learning in mice lacking NMDA receptor epsilon1 subunit. *Nature*. **373**, 151–155 (1995).
74. Tang, Y. P. et al. Genetic enhancement of learning and memory in mice. *Nature*. **401**, 63–69 (1999).
75. Rioult-Pedotti, M. S., Friedman, D., Donoghue, J. P. & Learning-induced, L. T. P. in neocortex. *Science* **290**, 533–536 (2000).
76. Dumitriu, D. et al. Selective changes in thin spine density and morphology in monkey prefrontal cortex correlate with aging-related cognitive impairment. *J. Neurosci* **30**, 7507–7515 (2010).
77. Morrison, J. H. & Baxter, M. G. The ageing cortical synapse: hallmarks and implications for cognitive decline. *Nat. Rev. Neurosci.* **13**, 240–250 (2012).
78. Morrison, J. H. & Hof, P. R. Life and death of neurons in the aging cerebral cortex. *Int. Rev. Neurobiol.* **81**, 41–57 (2007).
79. Cooke, S. F. & Bliss, T. V. Long-term potentiation and cognitive drug discovery. *Curr Opin Investig Drug* **6**(1), 25–34 (2005).
80. Molecular Basis of Nutrition and Aging: A Volume in the Molecular Nutrition Series. *Proceedings of the Elsevier Inc.* 2016.
81. Fernandez, A. M. & Torres-Aleman, I. The many faces of insulin-like peptide signalling in the brain. *Nat. Rev. Neurosci.* **13**, 225–239 (2012).
82. Kim, S. J. & Han, Y. Insulin inhibits AMPA-induced neuronal damage via stimulation of protein kinase B (Akt). *J. Neural Transm* **112**, 179–191 (2005).
83. Dudek, H. et al. Regulation of neuronal survival by the serine-threonine protein kinase Akt. *Science* **275**, 661–665 (1997).
84. Carro, E. & Torres-Aleman, I. The role of insulin and insulin-like growth factor I in the molecular and cellular mechanisms underlying the pathology of Alzheimer's disease. *Eur. J. Pharmacol.* **490**, 127–133 (2004).
85. Fernandez, A. M., Fernandez, S., Carrero, P., Garcia-Garcia, M. & Torres-Aleman, I. Calcineurin in reactive astrocytes plays a key role in the interplay between proinflammatory and anti-inflammatory signals. *J. Neurosci* **27**, 8745–8756 (2007).
86. Feil R., Metzger D. *Conditional mutagenesis: an approach to disease models*, vol. 178. Springer Science & Business Media 2007.
87. Werner, H. & LeRoith, D. Insulin and insulin-like growth factor receptors in the brain: physiological and pathological aspects. *Eur Neuropsychopharmacol* **24**, 1947–1953 (2014).
88. Craft, S. et al. Intranasal insulin therapy for Alzheimer disease and amnesic mild cognitive impairment: a pilot clinical trial. *Arch. Neurol.* **69**, 29–38 (2012).
89. Liang, X., Zou, Q., He, Y. & Yang, Y. Coupling of functional connectivity and regional cerebral blood flow reveals a physiological basis for network hubs of the human brain. *Proc Natl Acad Sci* **110**, 1929–1934 (2013).
90. Riedl, V. et al. Metabolic connectivity mapping reveals effective connectivity in the resting human brain. *Proc Natl Acad Sci* **113**, 428–433 (2016).
91. Mintun, M. A. et al. Distribution of glycolysis in the resting healthy human brain correlates with distribution of beta-amyloid plaques in Alzheimer's disease. *Soc. Neurosci. Abstr.* **707** (2006).
92. Perantie, D. C. et al. Regional brain volume differences associated with hyperglycemia and severe hypoglycemia in youth with type 1 diabetes. *Diabetes. Care*. **30**, 2331–2337 (2007).
93. García-Casares, N. et al. Structural and functional brain changes in middle-aged type 2 diabetic patients: a cross-sectional study. *J. Alzheimer's Dis* **40**, 375–386 (2014).
94. Musen, G. et al. Resting-state brain functional connectivity is altered in type 2 diabetes. *Diabetes*. **61**, 2375–2379 (2012).
95. Chen Y et al. Selectively disrupted functional connectivity networks in type 2 diabetes mellitus. *Front Aging Neurosci* **7**, 233 (2015).
96. Snyder, H. R. et al. Neural inhibition enables selection during language processing. *Proc Natl Acad Sci U S A* **107**, 16483–16488 (2010).
97. Banuelos, C. et al. Prefrontal cortical GABAergic dysfunction contributes to age-related working memory impairment. *J. Neurosci* **34**, 3457–3466 (2014).
98. Menard, C. & Quirion, R. Group 1 metabotropic glutamate receptor function and its regulation of learning and memory in the aging brain. *Front Pharmacol* **3**, 182 (2012).
99. Glorioso, C. & Sibille, E. Between destiny and disease: genetics and molecular pathways of human central nervous system aging. *Prog. Neurobiol.* **93**, 165–181 (2011).
100. Mattson, M. P., Chan, S. L. & Duan, W. Modification of brain aging and neurodegenerative disorders by genes, diet, and behavior. *Physiol. Rev.* **82**, 637–672 (2002).
101. Zhen, X., Uryu, K., Cai, G., Johnson, G. P. & Friedman, E. Age-associated impairment in brain MAPK signal pathways and the effect of caloric restriction in Fischer 344 rats. *J. Gerontol. A. Biol. Sci. Med. Sci.* **54**, B539–548 (1999).
102. Tapia-Arancibia, L., Aliaga, E., Silhol, M. & Arancibia, S. New insights into brain BDNF function in normal aging and Alzheimer disease. *Brain. Res. Rev.* **59**, 201–220 (2008).
103. Bernal, G. M. & Peterson, D. A. Phenotypic and gene expression modification with normal brain aging in GFAP-positive astrocytes and neural stem cells. *Aging. Cell*. **10**, 466–482 (2011).
104. Dityatev A., El-Husseini A. *Molecular Mechanisms of Synaptogenesis*. Springer US 2006.
105. Wang, D. D. & Kriegstein, A. R. GABA regulates excitatory synapse formation in the neocortex via NMDA receptor activation. *J. Neurosci* **28**, 5547–5558 (2008).
106. Oh, W. C., Lutz, S., Castillo, P. E. & Kwon, H. B. De novo synaptogenesis induced by GABA in the developing mouse cortex. *Science* **353**, 1037–1040 (2016).
107. Lee, HuangC. C. & Hsu, K. S. Insulin promotes dendritic spine and synapse formation by the PI3K/Akt/mTOR and Rac1 signaling pathways. *Neuropharmacology*. **61**, 867–879 (2011).
108. Oishi, K. et al. Selective induction of neocortical GABAergic neurons by the PDK1-Akt pathway through activation of Mash1. *Proc Natl Acad Sci U S A* **106**, 13064–13069 (2009).
109. Reuter-Lorenz, P. A. & Park, D. C. Human neuroscience and the aging mind: a new look at old problems. *J. Gerontol. B. Psychol. Sci. Soc. Sci.* **65**, 405–415 (2010).